Supporting Information

A microporous anionic metal–organic framework for highly selective and sensitive electrochemical sensor of Cu^{2+} ion

J. C. Jin,[a,b,#] J. Wu,[a,b,#] G. P. Yang,[a] Y. L. Wu[a] and Y. Y. Wang*[a]

[a]*Key Laboratory of Synthetic and Natural Functional Molecule Chemistry of the Ministry of Education, Shaanxi Key Laboratory of Physico-Inorganic Chemistry, College of Chemistry & Materials Science, Northwest University. Xi'an 710069, China.*

[b]*Technology Promotion Center of Nano Composite Material Preparation and Application; Anhui Provincial Laboratory of Biomimetic Sensor and Detecting Technology, West Anhui University, Anhui 237012 , China.*

 # These authors contributed equally to this work.

Materials and Measurements. All reagents and solvents were commercially available and were used without further purification. The solutions were prepared with 18 mΩ• cm ultrapure water. All glassware was cleaned prior to use by sequential washing in 1M HCl and 1M HNO_3, followed by a thorough rinsing with ultrapure water. Infrared spectra were obtained in KBr discs on a Nicolet Avatar 360 FTIR spectrometer in the 400-4000 cm^{-1} region. Photoluminescence analyses were performed on an Edinburgh FLS55 luminescence spectrometer. Elemental analyses (C, H and N) were performed with a Perkin Elmer 2400C Elemental Analyzer. Thermalgravimetric analyses (TGA) were carried out in nitrogen stream using a Netzsch TG209F3 equipment at a heating rate of 5°C/min. Powder X-ray diffraction (PXRD) data were recorded on a Bruker D8 ADVANCE X-ray powder diffractometer (Cu Kα, 1.5418 Å). Electrochemical measurements were performed using a conventional three-electrode system with the Au/Me_2NH_2@MOF-1 modified glassy carbon working electrode (CHI104), a Pt wire counter electrode, and Hg/Hg_2Cl_2 (3 M KCl) reference electrode. Cyclic voltammograms and SWASV were recorded using a computer controlled CHI660E electrochemical analyzer (CH Instruments, Shanghai, China).

Crystallography. The diffraction data was collected at 295(2) and 100(2) K for Me_2NH_2@MOF-1, with a Bruker-AXS SMART CCD area detector diffractometer using ω rotation scans with a scanwidth of 0.3º and Mo Kα radiation (λ = 0.71073 Å). Absorption corrections were carried out utilizing SADABS routine.[1] The structures were solved by direct methods and refined using the SHELXTL 97 software.[2] Atoms were located from iterative examination of difference Fmaps following least squares refinements of the earlier models. All the atoms except hydrogen atoms, which were fixed at calculated positions and refined by using a riding mode, were refined anisotropically until full convergence was achieved. It was necessary to constrain or restrain a number of bond lengths and angles in the structure in order get a stable refinement and chemically reasonable model. The crystallographic data and selected bond lengths and angles for Me_2NH_2@MOF-1 are listed in Table S2 and Table S3, respectively.

Synthesis of $[H_2N(CH_3)_2]_4[Zn_3(Hdpa)_2]\cdot 4DMF$ (Me_2NH_2@MOF-1). A mixture of H_6dpa (48.4 mg, 0.10 mmol) and $Zn(CH_3COOH)_2\cdot 2H_2O$ (44.4 mg, 0.20 mmol) was dissolved in DMF (2 mL) in a screw-capped vial. After one drops of HNO_3 (62%, aq.) and 0.5 mL of H_2O were added to the mixture, the vial was capped and placed in an oven at 105 ºC for 6 days. The resulting single crystals were washed with DMF three times to give Me_2NH_2@MOF-1. Anal. Calc. for $C_{68}H_{78}Zn_3N_8O_{28}$: C, 49.45; H, 4.76; N, 6.78. Found: C, 48.74; H, 5.02; N, 6.96%. IR (KBr, cm^{-1}, Figure S9): 3423(m), 3063(w), 2793(s), 2502(m), 2150(w), 1656(m), 1614(s), 1442(m), 1338(s), 1094(m), 1021(m), 780(s), 717(m), 630(m), 567(m), 514(m), 420(w).

Preparation Me_2NH_2@MOF-1 Modified Electrode. An adapted preparation method based on previous report was used to prepare the Au/Me_2NH_2@MOF-1/GCE. [3,4] Before the experiment, a commercial GCE (3 mm diameter) was carefully polished with 0.05 mm Al_2O_3 powder on a polishing cloth to get a smoothly surface, and sequentially sonicated in 1:1 nitrate acid solution, 1M sodium hydroxide, acetone and double-distilled water for 5 minutes, respectively, then, dried at room temperature. After that the electrode was immersed in 0.005 M K_3 [$Fe(CN)_6$] containing 0.1 M KCl to scan cyclic voltammetry, and was ready to use once the difference between the oxidation and reduction peaks was less than 90 mV. Then, the GCE was carefully to rinse with ultrapure water and dried at room temperature. 100 mg Me_2NH_2@MOF-1were put into 100 mL ethanol and sonicated for 5 min to obtain a uniform dispersion suspension. 5 L of the above Me_2NH_2@MOF-1 suspension was straight dispersed onto the fresh surface of GCE and dried at room temperature. After evaporation of ethanol, a thin Me_2NH_2@MOF-1 film was formed on the electrode surface.

The preparation for the in situ deposition of gold nanoparticles at Me_2NH_2@MOF-1/GCE was modified according to previous publication. [3, 4] The Me_2NH_2@MOF-1 was immerged into 1 mM $HAuCl_4$ and 0.5 M H_2SO_4 solutions, then the electrodeposition was performed by five cyclic voltammetry steps in the potential range from +1.5 V to -0.6 V at a scan rate of 100 mV/s for every

one minute. After being cleaned with ethanol, ultrapure water, the AuNPs/ Me_2NH_2@MOF-1 modified GCE was dried at room temperature and formed the AuNPs/ Me_2NH_2@MOF-1/GCE, and then, rinsed with ultrapure water before being used for the detection of copper (II).

Electrochemical measurements. Copper(II) was chemically preconcentrated by immersing the AuNPs/ Me_2NH_2@MOF-1/GCE in the solution containing copper (II) for 30 min in an open circuit. During preconcentration, the solution was efficiently stirred (above 500 rpm). The electrode was taken out, and thoroughly washed with water and then kept in a cell containing 20 mL of supporting electrolyte solution (0.05 M KCl). A negative potential of −0.4 V was applied to the electrode immediately for 120 s to reduce copper (II) into elemental metallic copper. Subsequently, the square wave anodic stripping voltammetry (SW ASV) measurements were performed in the potential range from −0.4 to +0.60V with a frequency of 60 Hz, amplitude of 25 mV, and a potential step of 4mV. After the measurements, the electrode was regenerated by immersing in a stirring solution containing 0.2M HNO_3 at +0.8V for 60 s. The renewed electrode then was checked in the supporting electrolyte before the next measurement to ensure that it did not show any peak within the potential range. The electrochemical impedance spectroscopy was scanned in 0.01M $Fe(CN)_6^{3-/4-}$ and 0.1M KCl solution at the formal potential of 0.25V with a frequency range of 0.01–105 Hz and a signal amplitude of 5mV. All measurements were performed at room temperature.

References

[1] Bruker. SADABS, SMART and SAINT. Bruker AXS Inc., Madison, Wisconson, USA, **2002**.

[2] G. M. Sheldrick, SHELXL-97, program for the refinement of the crystal structures. University of Göttingen, Germany, **1997**.

[3] X. C. Fu, J. Wu , J. Li , C. G. Xie, Y. S. Liu, Y. Zhong, J. H. Liu, *Sensor Actuat B-Chem.* **2013**, *182*, 382-389.

[4] J.Wu, M. Yang, J. Xiao, X. C. Fu, J. C. Jin, L. G. Li, W. G. Chang, C. G. Xie, *J. Electrochem. Soc.* **2013**, *160*, B225-B230.

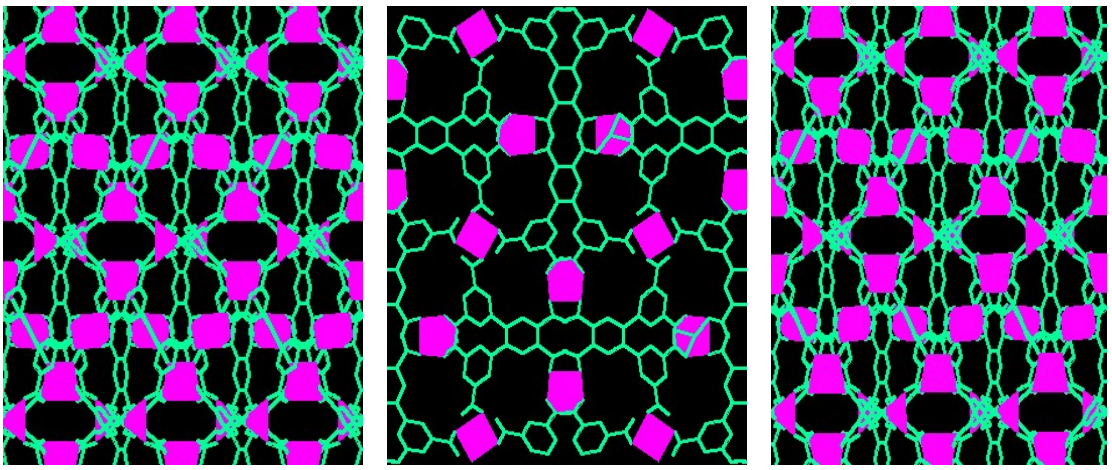

Fig S1: The microporous characteristic of Me_2NH_2@MOF-1 in ab, ac, bc planes respectively.

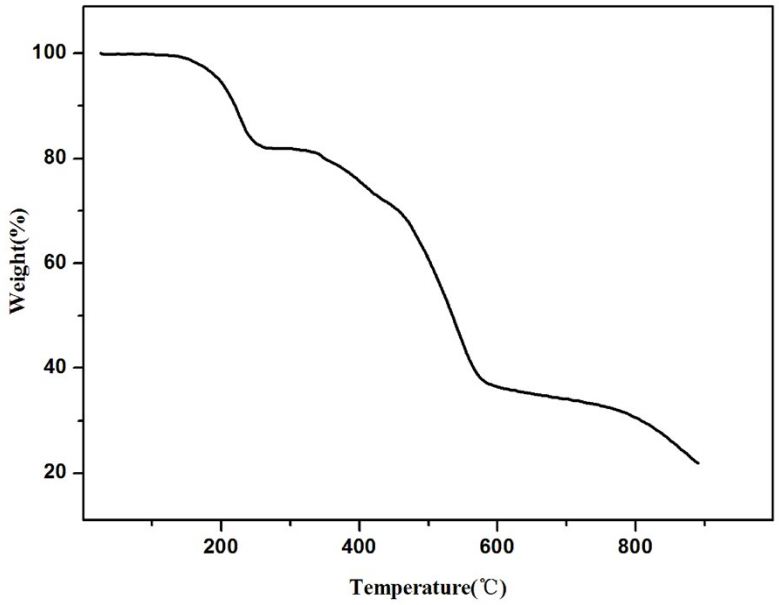

Fig S2: TGA plot of Me_2NH_2@MOF-1 under N_2 environment. Thermogravimetric analysis (TGA) reveals that Me_2NH_2@MOF-1 can be stable up to 300℃. In the temperature range 120–260 ºC, there is loss of all the guest DMF molecules (obsd: 17.68%, calcd: 18.06%). From 260 to 300 ºC, the TGA curve of **1** passes through a flat area, and then the decomposition of framework.

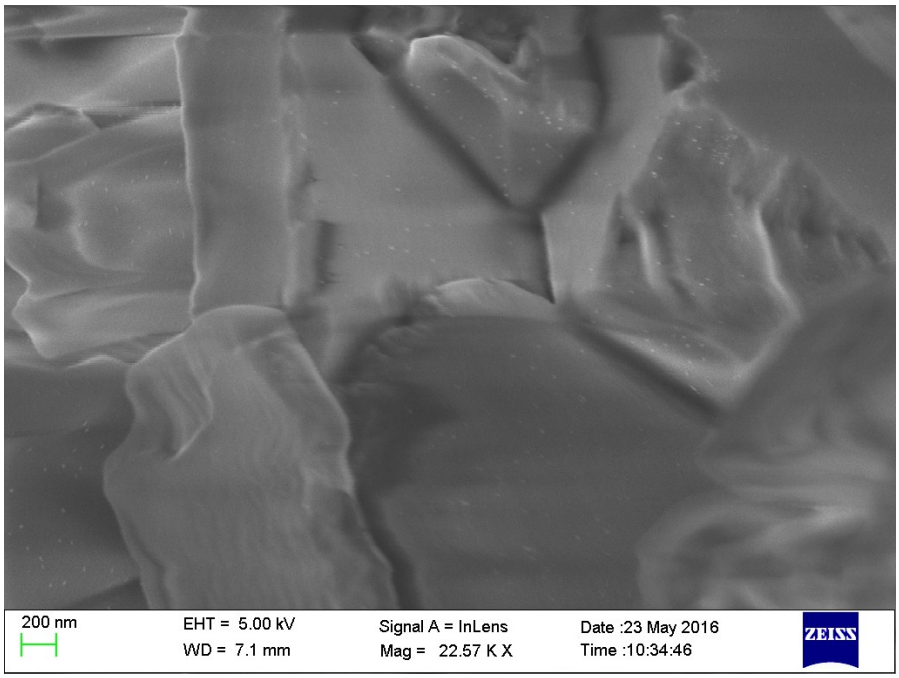

Fig S3: FESEM images of the Me_2NH_2@MOF-1 after the electrodeposition of AuNPs.

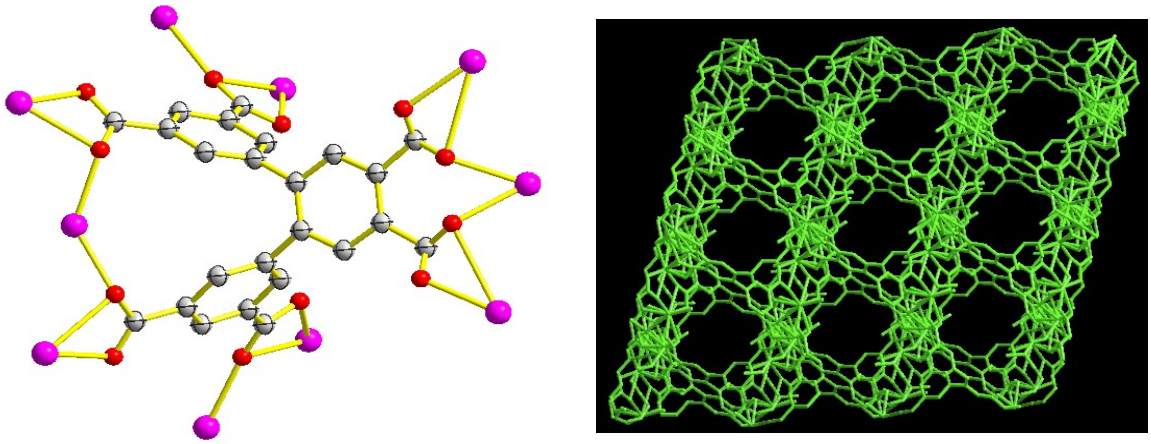

Fig S4: The deprotonated ligand and the microporous neutral metal-organic framework in MOF-1′.

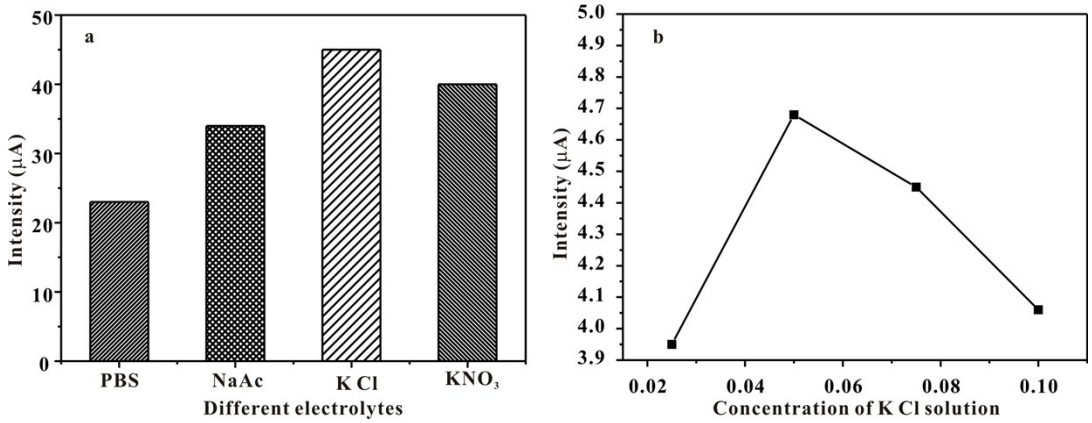

Fig S5: (a) The relative SWASV signal (μA) (background current was subtracted) response of the Au/Me_2NH_2@MOF-1/GCE by different electrolytes in 7×10^{-8} M copper (II) solution; (b) The relative SWASV signal (μA) (background current was subtracted) response of the Au/Me_2NH_2@MOF-1/GCE in different concentration of KCl in a 7×10^{-8} M copper (II) solution (with immersing time of 30 minutes and reduction time of 100 seconds. SWASV conditions: Frequency 40 Hz, amplitude 20 mV, potential increment 4mV).

The supporting electrolyte has a fateful influence on the extraction and determination steps of copper (II) ions, and the KCl, PBS, NaAc, KNO_3 electrolytes were studied. Fig S5a shows the relative SWASV signal response of the Au/Me_2NH_2@MOF-1/GCE modified electrode to copper (II) (1.0×10^{-8} M) in varying supporting electrolytes, respectively. A maximum signal response was observed when 0.05 M KCl was used as electrolytes. To investigate the influence of the concentration of the solution matrix, the 0, 0.025, 0.05, 0.075 and 0.10 M KCl electrolytes were also studied. Fig S5b shows the relative SWASV signal response of the Au/Me_2NH_2@MOF-1/GCE modified electrode in different concentration of KCl solution. A maximum signal response was observed when 0.05 M KCl was used as electrolytes. Thus, we selected the 0.05 M KCl solution as the solution matrix.

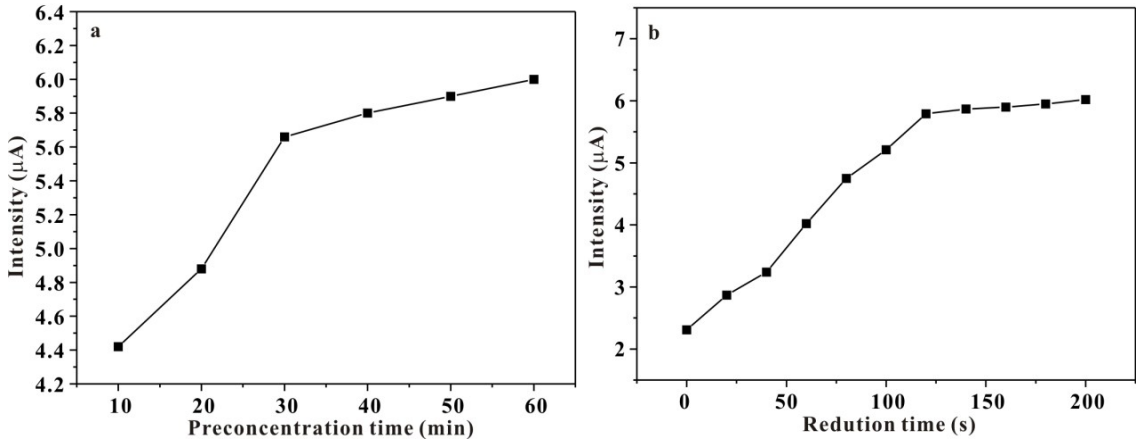

Fig S6: (a) The relative SWASV signal response of the Au/ Me_2NH_2@MOF-1/GCE in 1×10^{-11} M copper (II) solution (with reduction time of 100 seconds. SWASV conditions: Frequency 40 Hz, amplitude 20 mV, potential increment 4mV); (b) The relative SWASV signal response of the Au/Me_2NH_2@MOF-1/GCE with different reduction time in a 1×10^{-9} M copper (II) solution (with preconcentration time of 30 minutes. SWASV conditions: Frequency 40 Hz, amplitude 20 mV, potential increment 4mV).

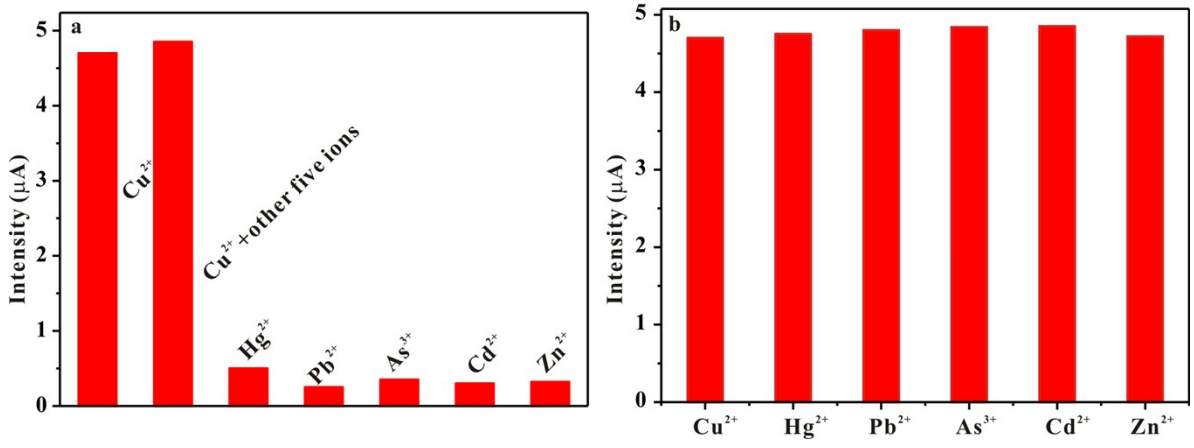

Fig S7: (a) Typical SWASV signals (μA) for 1.0×10^{-10} M of Cu^{2+}, Cu^{2+} added the other five ions, Hg^{2+}, Pb^{2+}, As^{3+}, Cd^{2+}, and Zn^{2+} by the Au/Me_2NH_2@MOF-1/GCE in 0.1 M KCl electrolyte, respectively (with reduction time of 100 seconds and immersing time of 30 minutes. SWASV conditions: Frequency 40 Hz, amplitude 20 mV, potential increment 4mV); (b) The relative SWASV signal response of 1.0×10^{-10} M copper at the Au/Me_2NH_2@MOF-1/GCE in the presence of a 10-fold molar excess of Hg^{2+}, Pb^{2+}, As^{3+}, Cd^{2+}, and Zn^{2+}, respectively (with reduction time of 100 seconds and

immersing time of 30 minutes. SWASV conditions: Frequency 40 Hz, amplitude 20 mV, potential increment 4mV).

The electrochemical signal response in the presence of the representative metallic ions including Hg^{2+}, Pb^{2+}, As^{3+}, Cd^{2+}, and Zn^{2+} was performed under the optimization of the conditions . Remarkably, these tested ions had no effect on the intensity of the electrochemical signal response of the Au/Me_2NH_2@MOF-1/GCE (see Fig S7a). The response of Au/Me_2NH_2@MOF-1/GCE electrochemical sensor to copper was almost unchanged before and after the addition of other interfering ions as illustrated in Fig S7b. When detecting copper using Au/Me_2NH_2@MOF-1/GCE the tolerance concentrations of other ions (Hg^{2+}, Pb^{2+}, As^{3+}, Cd^{2+}, and Zn^{2+}) were at least 10 times higher than that of copper (II).

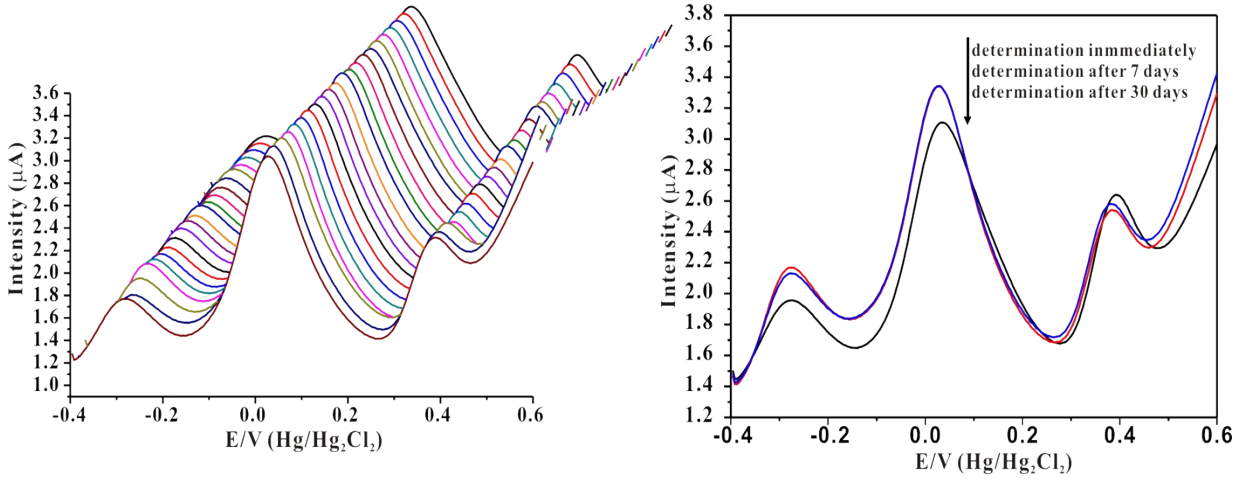

Fig S8: (a) The relative SWASV signal response of the Au/Me_2NH_2@MOF-1/GCE in 1×10^{-11} M copper (II) solution for 23 times (with preconcentration time of 30 minutes and reduction time of 100 seconds. SWASV conditions: Frequency 40 Hz, amplitude 20 mV, potential increment 4mV); (b) The relative SWASV signal response of the Au/Me_2NH_2@MOF-1/GCE for determination 1×10^{-11} M copper (II) solution in different time interval storage (with preconcentration time of 30 minutes and reduction time of 100 seconds. SWASV conditions: Frequency 40 Hz, amplitude 20 mV, potential increment 4mV).

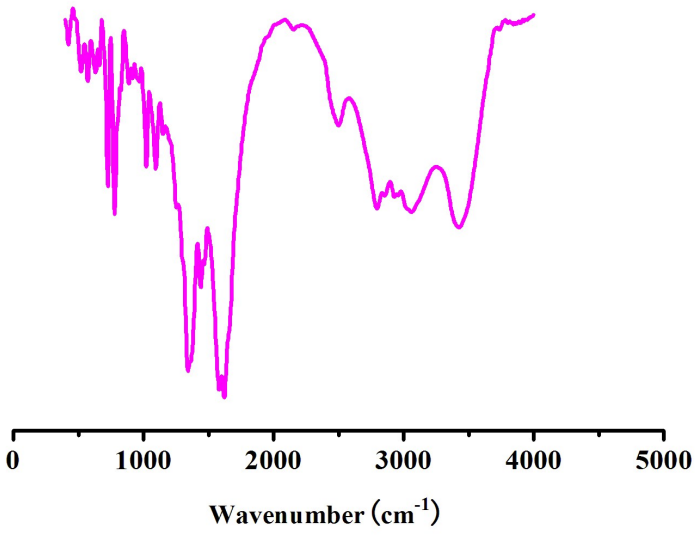

Fig S9: The IR patterns of Me_2NH_2@MOF-1

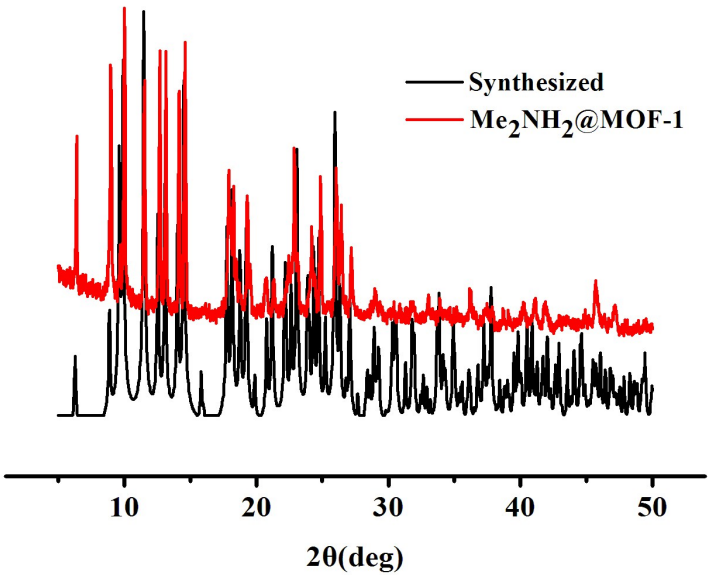

Fig S10: The XPRD patterns of complex Me_2NH_2@MOF-1.

The X-ray powder diffraction (XRPD) patterns of Me_2NH_2@MOF-1 were checked at room temperature, although minor differences can be seen in the positions, intensities, and widths of some peaks, which indicates that Me_2NH_2@MOF-1 were obtained as a single phase.

Table S1. Analytical results of Cu^{2+} in the Pihe river water samples using the proposed method (n = 3)

Sample	Original (M)	Added (M)	Found (M)	Recovery (%)	RSD(%)
River water 1	2.17×10^{-8}	2.00×10^{-8}	4.51×10^{-8}	108.2	2.6
River water 2	2.17×10^{-8}	4.00×10^{-8}	6.31×10^{-8}	102.3	2.8
River water 3	2.17×10^{-8}	1.00×10^{-7}	1.194×10^{-7}	98.1	2.7

The river water sample was collected from Pihe River (3:00 PM, May 10th, 2015, Lu'an, City, Anhui, China). It was first pretreated by a standard 0.45 μm filter and then was added with copper (II) at different concentration levels (2.0×10^{-8}–1.0×10^{-7} M). The original copper (II) concentration in Pihe River water sample was found to be 2.17×10^{-8} M (RSD, 2.5%) using Au/Me_2NH_2@MOF-1/GCE sensor determination before the addition of copper (II), and a value of 23.8±0.02 nM was obtained by ICPMS, showing a difference of 8.9%.

Table S2. Selected crystallographic data for Me_2NH_2@MOF-1

Compound	**Me_2NH_2@MOF-1**
Empirical formula	$C_{68}H_{78}Zn_3N_8O_{28}$
Formula mass	1651.49
Crystal system	tetragonal
Space group	I-42d
a [Å]	28.2219(17)
b [Å]	28.2219(17)
c [Å]	9.7266(12)
α/(°)	90
β/(°)	90
γ/(°)	90
Dx,g cm^{-3}	1.416
Nref	3499
V [$Å^3$]	7747.0(13)
Z	4
Tmin, Tmax	0.767, 0.877
S	1.043
μ [mm^{-1}]	1.006
F [000]	3424.0
Reflections collected	3157
Final *R*[a] indices [I>2σ(I)]	R_1 = 0.0548 wR_2 = 0.1507

[a] $R_1=\sum||F_o|-|F_c||/\sum|F_o|$, $wR_2=[\sum w(F_o^2-F_c^2)^2/\sum w(F_o^2)^2]^{1/2}$

Table S3. Selected bond lengths (Å) and angles (˚) of Me_2NH_2@MOF-1

Me_2NH_2@MOF-1			
Zn(1)-O(2)	1.9616(30)	Zn(1)-O2(A)	1.9616(30)
Zn(1)-O2(B)	1.9616(30)	Zn(1)-O2(C)	1.9616(30)
O(2)-Zn(1)-O2(A)	100.477(124)	O(2)-Zn(1)-O2(B)	129.518(117)
O(2)-Zn(1)-O2(C)	100.477(124)	O2(A)-Zn(1)-O2(B)	100.477(124)
O2(A)-Zn(1)-O2(C)	129.518(117)	O2(B)-Zn(1)-O2(C)	100.477(124)
Zn(2)-O(3)	2.0359(37)	Zn(2)-O(4)	2.4048(62)
Zn(2)-O4(D)	2.4048(62)	Zn(2)-O3(D)	2.0359(37)
Zn(2)-O5(F)	1.9970(31)	Zn(2)-O5(E)	1.9970(31)
O(3)-Zn(2)-O(4)	57.545(176)	O(3)-Zn(2)-O4(D)	90.356(171)
O(3)-Zn(2)-O3(D)	137.748(133)	O(3)-Zn(2)-O5(F)	109.627(117)
O(3)-Zn(2)-O5(E)	95.511(127)	O(4)-Zn(2)-O4(D)	85.244(202)
O(4)-Zn(2)-O3(D)	90.356(171)	O(4)-Zn(2)-O5(F)	89.722(167)
O(4)-Zn(2)-O5(E)	152.459(168)	O4(D)-Zn(2)-O3(D)	57.545(176)
O4(D)-Zn(2)-O5(F)	152.459(168)	O4(D)-Zn(2)-O5(E)	89.722(167)
O3(D)-Zn(2)-O5(F)	95.511(127)	O3(D)-Zn(2)-O5(E)	109.627(117)
O5(F)-Zn(1)-O5(E)	106.374(125)		

[a] Symmetry codes: A 0.5+y, 0.5-x, 1.5-z; B 1-x, -y, z; C 0.5-y, -0.5+x, 1.5-z; D x, 0.5-y, 0.25-z; E 0.5-y, -0.5+x, 0.5-z; F 0.5-y, 1-x, -0.25+z.